

Dimerization of a copper(II) compound with a tetradentate diaminodiamide ligand †

Peter Comba,^{*a} Sergey P. Gavrish,^b Yaroslaw D. Lampeka,^b Philip Lightfoot^c and Alexander Peters^a

^a Anorganisch-Chemisches Institut der Universität Heidelberg, Im Neuenheimer Feld 270, D-69120 Heidelberg, Germany. Fax: +49 6221-54 66 17; E-mail: comba@akcomba.oci.uni-heidelberg.de

^b L. V. Pisarzhevskii Institute of Physical Chemistry of the National Academy of Sciences of the Ukraine, Prospekt Nauki 31, 252039 Kiev, Ukraine

^c School of Chemistry, University of St. Andrews, Purdie Building, St. Andrews, Fife, UK KY16 9ST

Received 6th July 1999, Accepted 27th September 1999

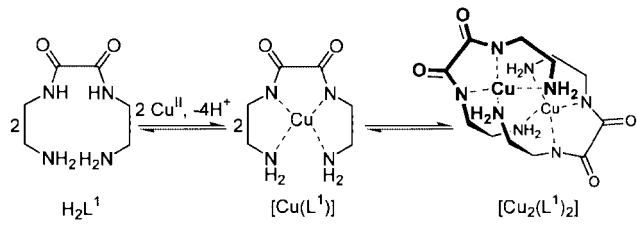
Two types of crystals were isolated from aqueous solutions of copper(II) salts, the tetradentate diaminodiamide ligand H_2L^1 ($H_2L^1 = 1,8\text{-diamino-3,6-diazaoctane-4,5-dione}$) and base. Crystal structural analyses revealed that one is the expected $[Cu(L^1)]$ and the other is the corresponding dimer $[Cu_2(L^1)_2]$, with the two copper(II) chromophores in nearly parallel planes ($Cu \cdots Cu$ distance = 3.35 Å; angle between the two planes, $\theta = 18.6^\circ$), where each ligand coordinates to both metal centers. Relief of strain, induced by the central, flat, five-membered chelate ring with two amide donors and two fused five-membered rings, and van der Waals attractions may be responsible for the stabilization of the dimer. This is supported by force field calculations which accurately reproduce the experimentally observed structures (RMS = 0.14 (monomer), 0.19 Å (dimer)), define them as the lowest strain energy conformers and find a stabilization of the dimer by 24 kJ mol⁻¹ ($\Delta U_{\text{strain}} = 2U_{\text{strain}}^{\text{monomer}} - U_{\text{strain}}^{\text{dimer}}$).

Introduction

Studies of di- and oligo-nuclear transition metal compounds are getting more and more popular, due to the increasing interest in and understanding of metalloprotein active sites, of co-operative effects in catalysis and of magnetic, electrochemical and spectroscopic effects of electronically coupled oligonuclear transition metal compounds, and due to their relevance in supramolecular systems and materials science.^{1–6}

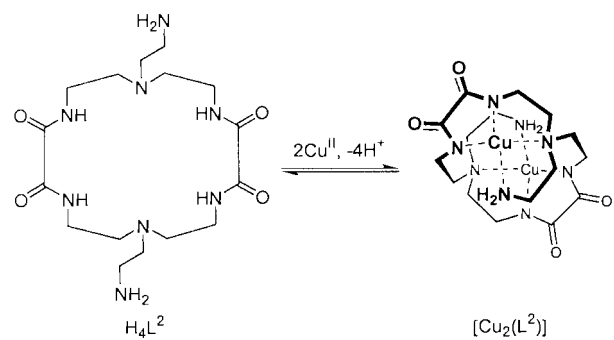
Relatively few dinuclear systems are known which result from dimerization of mononuclear building blocks, for which the thermodynamics of the dimerization process has been studied and where the structures of both the monomeric and dimeric forms have been determined. Detailed information on this type of process is also of interest for understanding the principles of molecular self-organization. The assembly of oligonuclear systems requires neutralization of the charges of the metal cations, and published systems are generally based on complexes of anionic ligands (e.g. carboxylates).^{7–10} Dimerization leads to a loss of entropy, and the driving force for the formation of dinuclear compounds may involve relief of steric strain and optimization of electronic effects, electrostatic interactions, hydrogen bonding and van der Waals interactions. Non-covalent interactions are particularly far reaching forces and attractive over a large range of distances, and therefore especially important for the assembly of di- and oligo-nuclear compounds.^{11,12}

We report here the synthesis and structural characterization of the mononuclear copper(II) compound $[Cu(L^1)]$ ($H_2L^1 = 1,8\text{-diamino-3,6-diazaoctane-4,5-dione}$) and of its dimer, $[Cu_2(L^1)_2]$, see Scheme 1. The diaminodiamide H_2L^1 leads to



Scheme 1

neutral metal complexes with dicationic metal ions and, due to the three fused five-membered chelate rings and the planarity and rigidity of the amide donors, to relatively strained compounds. A structurally similar octadentate ligand system H_4L^2 was known to produce the dicopper(II) compound $[Cu_2(L^2)]$ ($L^2 = 7,16\text{-bis}(2\text{-aminoethyl)}\text{-}1,4,7,10,13,16\text{-hexaazacyclooctadecane-2,3,11,12-tetraonate}(4-)$; see Scheme 2) and its structure has been reported.¹³



Scheme 2

† Supplementary data available: rotatable 3-D crystal structure diagram in CHIME format. See <http://www.rsc.org/suppdata/dt/1999/4099/>

Results and discussion

Syntheses and molecular structures

The addition of stoichiometric amounts of copper(II) salts to an aqueous solution of H_2L^1 ($\text{pH} \approx 9.5$) yields a micro-crystalline precipitate of composition $\text{CuL}^1 \cdot 2\text{H}_2\text{O}$. The solution spectroscopic properties (see Experimental section) are consistent with a CuN_4 (amine/amide) chromophore; the comparably high value of the absorption coefficient suggests some distortion from planar geometry; the relatively high values for the ligand field transition energy as well as the values of A_{\parallel} and of g_{\parallel} indicate that there is no substantial axial interaction (see Experimental section).^{14–16}

Single crystals, suitable for X-ray diffraction, were obtained from saturated aqueous solutions, covered with a layer of acetone. Two types of crystals, purple cubes of $[\text{Cu}_2(\text{L}^1)] \cdot 6\text{H}_2\text{O}$, insoluble in common organic solvents and only slightly soluble in water, and purple needles of $[\text{Cu}(\text{L}^1)] \cdot 2\text{H}_2\text{O}$, soluble in water and DMF, were isolated and structurally characterized. UV-vis reflectance spectra indicated that the chromophores of the two materials are virtually identical and similar to that observed in solution for $[\text{Cu}(\text{L}^1)]$ ($\tilde{\nu}_{\text{max}}/\text{cm}^{-1}$: 18200 (dimer) vs. 18800 (monomer) vs. 18900 (solution), see Experimental section). Selected bond distances and valence angles of $[\text{Cu}(\text{L}^1)] \cdot 2\text{H}_2\text{O}$ and $[\text{Cu}_2(\text{L}^1)] \cdot 6\text{H}_2\text{O}$ are collected in Table 1 and perspective views of the two compounds with the atom numbering schemes are shown in Fig. 1.

The monomer, $[\text{Cu}(\text{L}^1)] \cdot 2\text{H}_2\text{O}$, has a square planar CuN_4 chromophore (RMS deviation of the donors from the least squares plane of the nitrogen atoms 0.005 Å). The $\text{Cu}-\text{N}_{\text{amide}}$ distances are, as expected, considerably shorter than the $\text{Cu}-\text{N}_{\text{amine}}$ bond lengths (1.93 vs. 2.02 Å, see Table 1).¹⁶ The two lateral five-membered chelate rings have different conformations, one is a flattened envelope (distances of C(5) and C(6) from the $\text{CuN}(3)\text{N}(4)$ plane: −0.05, −0.58 Å), the other is *gauche* (distances of C(1) and C(2) from the $\text{CuN}(1)\text{N}(2)$ plane: −0.41, +0.11 Å). Noteworthy are the small N–C–C–N torsion

angles of 40° for these two chelate rings. A network of hydrogen bonds that involves the carbonyl oxygen atoms, the amine protons and water molecules links the molecular complexes into linear aggregates, where the complexes have alternating orientations, rotated by 180°.

The dimer $[\text{Cu}_2(\text{L}^1)]_2 \cdot 6\text{H}_2\text{O}$ is formed by opening one of the lateral chelate rings in the monomer and binding the resulting pendant amine to a vacant in-plane co-ordination site of a neighboring copper center. There are various possible isomers and that observed experimentally is the most stable structure (see below). It has pseudo- C_2 symmetry (folded structure, the two diamide donor groups have *anti* orientation); the chromophores are similar to that of the monomer. The RMS deviations of the donors from the N_4 best planes are approximately 0.05 Å for both chromophores and those of the copper centers are 0.09 Å. The two best planes are tilted by 18.6° and the $\text{Cu} \cdots \text{Cu}$ distance is 3.353 Å. The two five-membered chelate rings involving the amine donors have envelope conformations (N–C–C–N torsion angles of 36°). The most significant structural differences between the chromophores of the monomer and the dimer are the relative $\text{Cu}-\text{N}_{\text{amine}}$ and $\text{Cu}-\text{N}_{\text{amide}}$ distances (monomer vs. dimer: $\text{Cu}-\text{N}_{\text{amine}}$ 2.03 vs. 2.06 (chelate), 1.98 (terminal); $\text{Cu}-\text{N}_{\text{amide}}$ 1.93 vs. 2.00 (terminal), 1.92 Å (chelate)). A pattern similar to that in the dimer was found in the dicopper(II) complex of a dinucleating macrocycle with analogous chromophores ($[\text{Cu}_2(\text{L}^2)]$, Scheme 2, see below).¹³

Molecular modeling

The formation of $[\text{Cu}_2(\text{L}^1)]_2$ is a dimerization, that is $[\text{Cu}_2(\text{L}^1)]_2$ and $2[\text{Cu}(\text{L}^1)]$ are isomeric systems. Thus, the steric energies of the two species are relevant in terms of the relative stability of the dimer, and molecular mechanics should be able to identify possible reasons for the stabilization of the dinuclear compound.

The crystal structural co-ordinates of $[\text{Cu}(\text{L}^1)] \cdot 2\text{H}_2\text{O}$ and $[\text{Cu}_2(\text{L}^1)] \cdot 6\text{H}_2\text{O}$ were used as starting structures for a conformational analysis. There is only limited conformational flexibility and all local minima are very close in energy; the lowest energy structures, based on the MOMEc force field,¹⁸ are shown in Fig. 2 and the corresponding strain energies are

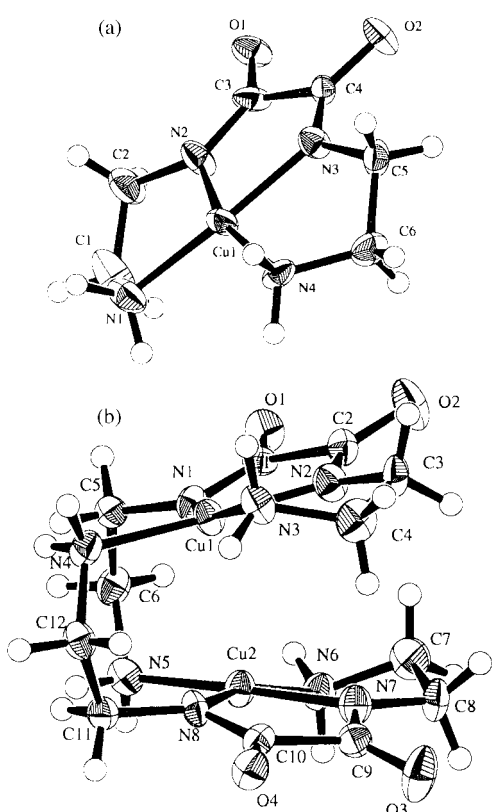


Fig. 1 The ORTEP¹⁷ plots of the complexes (a) $[\text{Cu}(\text{L}^1)] \cdot 2\text{H}_2\text{O}$, (b) $[\text{Cu}_2(\text{L}^1)] \cdot 6\text{H}_2\text{O}$; water molecules omitted for clarity.

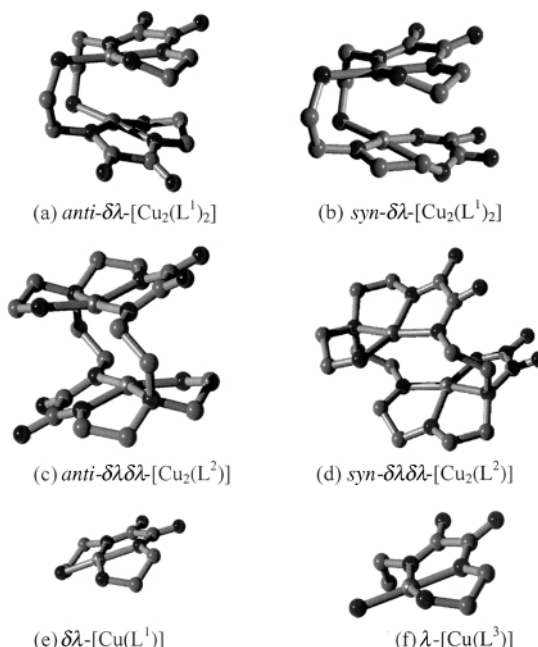


Fig. 2 Diagrams of the strain energy optimized structures (lowest energy conformers): (a) $\text{anti-}\delta\lambda\text{-}[\text{Cu}_2(\text{L}^1)]_2$, (b) $\text{syn-}\delta\lambda\text{-}[\text{Cu}_2(\text{L}^1)]_2$, (c) $\text{anti-}\delta\lambda\delta\lambda\text{-}[\text{Cu}_2(\text{L}^2)]$, (d) $\text{syn-}\delta\lambda\delta\lambda\text{-}[\text{Cu}_2(\text{L}^2)]$, (e) $\delta\lambda\text{-}[\text{Cu}(\text{L}^1)]$, (f) $\lambda\text{-}[\text{Cu}(\text{L}^3)]$.

Table 1 Selected bond distances (Å) and angles (°) for $[\text{Cu}(\text{L}^1)] \cdot 2\text{H}_2\text{O}$ and $[\text{Cu}_2(\text{L}^1)_2] \cdot 6\text{H}_2\text{O}$

$[\text{Cu}(\text{L}^1)] \cdot 2\text{H}_2\text{O}$		$[\text{Cu}_2(\text{L}^1)_2] \cdot 6\text{H}_2\text{O}$		
Cu–N _{amine}	Cu–N(1)	2.033(7)	Cu(1)–N(3)	2.057(5)
	Cu–N(4)	2.018(7)	Cu(1)–N(4)	1.981(6)
Cu–N _{amide}	Cu–N(2)	1.924(7)	Cu(2)–N(5)	1.985(6)
	Cu–N(3)	1.941(7)	Cu(2)–N(6)	2.062(6)
Cu…Cu			Cu(1)–N(1)	1.995(5)
<i>cis</i> angles			Cu(1)–N(2)	1.917(6)
N _{amine} –Cu–N _{amine}	N(1)–Cu–N(4)	110.6(3)	Cu(2)–N(7)	1.915(6)
N _{amine} –Cu–N _{amide}	N(1)–Cu–N(2)	83.5(3)	Cu(2)–N(8)	2.008(5)
	N(3)–Cu–N(4)	83.5(3)	Cu(1)…Cu(2)	3.353
N _{amide} –Cu–N _{amide}	N(2)–Cu–N(3)	81.6(3)		
<i>trans</i> angles				
	N(1)–Cu–N(3)	163.9(3)	N(1)–Cu(1)–N(3)	162.5(2)
	N(2)–Cu–N(4)	164.2(3)	N(2)–Cu(1)–N(4)	174.1(2)
			N(5)–Cu(2)–N(7)	174.3(2)
			N(6)–Cu(2)–N(8)	162.0(2)
Tilt angle			Cu(1)N ₄ –Cu(2)N ₄	18.6
Torsion angles of all chelates				
	N(1)–C(1)–C(2)–N(3)	40.0(1)	N(1)–C(1)–C(2)–N(2)	1.4(8)
	N(2)–C(3)–C(4)–N(3)	0.0(1)	N(1)–C(5)–C(6)–N(5)	60.0(7)
	N(3)–C(5)–C(6)–N(4)	−40.0(1)	N(2)–C(3)–C(4)–N(3)	−36.1(8)
			N(4)–C(12)–C(11)–N(8)	61.9(7)
			N(6)–C(7)–C(8)–N(7)	36.8(8)
			N(7)–C(9)–C(10)–N(8)	2.3(8)

Table 2 Strain energies of the low energy conformations of $[\text{Cu}(\text{L}^1)]$, $[\text{Cu}_2(\text{L}^1)_2]$, $[\text{Cu}_2(\text{L}^2)]$ and $[\text{Cu}(\text{L}^3)]$ ^a

Conformation	Energy/kJ mol ^{−1}
$\delta\lambda$ - $[\text{Cu}(\text{L}^1)]$ (e)	32.4
$\delta\delta$ - $[\text{Cu}(\text{L}^1)]$	32.6
<i>anti</i> - $\delta\lambda$ - $[\text{Cu}_2(\text{L}^1)_2]$ (a)	41.2
<i>anti</i> - $\delta\delta$ - $[\text{Cu}_2(\text{L}^1)_2]$	42.2
<i>syn</i> - $\delta\lambda$ - $[\text{Cu}_2(\text{L}^1)_2]$ (b)	52.7
<i>anti</i> - $\delta\lambda\delta\lambda$ - $[\text{Cu}_2(\text{L}^2)]$ (c)	86.3
<i>syn</i> - $\delta\lambda\delta\lambda$ - $[\text{Cu}_2(\text{L}^2)]$ (d)	107.3
λ - $[\text{Cu}(\text{L}^3)]$ (f)	24.1

^a For structures see text and Fig. 2; the crystallographically observed conformations are (e), $\delta\lambda$ - $[\text{Cu}(\text{L}^1)]$, (a), *anti*- $\delta\lambda$ - $[\text{Cu}_2(\text{L}^1)_2]$, and (c), *anti*- $\delta\lambda\delta\lambda$ - $[\text{Cu}_2(\text{L}^2)]$.¹³

given in Table 2. Also included in Fig. 2 and Table 2 are the most stable conformers of $[\text{Cu}_2(\text{L}^2)]$ (see Scheme 2; the structurally characterized species has *anti* configuration), the *syn* isomers of $[\text{Cu}_2(\text{L}^1)_2]$ and $[\text{Cu}_2(\text{L}^2)]$, and of $[\text{Cu}(\text{L}^3)]$, a structure that corresponds to one half of the structure of *anti*- $[\text{Cu}_2(\text{L}^1)_2]$.

The most important result that emerges from Table 2 is that, based on the steric energies, the dimer is more stable than the monomer by 24 kJ mol^{−1}. The calculated strain energy of $[\text{Cu}(\text{L}^3)]$ (the strain energy minimized structure that represents one half of the dimer and also the putative chelate-ring-opened monomer) indicates that some of the stabilization (*i.e.* 16 kJ mol^{−1} per dimeric unit, that is 2/3 of the stabilization of the dimer) is due to the relaxation of strain that results from the three fused chelate rings in the monomer. The rest (*i.e.* 8 kJ mol^{−1} per dimeric unit) is due to attractive forces, mainly to van der Waals attraction. This also emerges from a thorough

inspection of all relevant energy terms of the optimized structures.

Note that our analysis does not include electrostatic forces but with neutral complexes these are expected to be of minor importance.¹⁹ We also stress that the energy differences are strongly dependent on the force field parameterization. However, it has been found that, in general, the MOMECC force field¹⁸ leads to reasonably accurate predictions of isomer equilibria.^{12,20,21} In particular, in structurally similar systems, there was good agreement between computed and experimentally observed isomer distributions.^{12,16,19,20} A third point to note is that the strain energies may be related to enthalpies and the entropy contribution to the dimerization process is not accounted for. Nevertheless, it would have been of interest to compare the strain energy differences with experimental thermodynamic data. This was not possible due to the low solubility of the dimer and the expectation that solutions of the monomer were not fully equilibrated (see solid state and solution electronic spectra).

Conclusion

The self-assembly of oligonuclear arrays is often based on a careful design of ligands. Their geometry, together with the metal-ion-based directionality of the metal–donor bonds, leads to the possibility to tune the three-dimensional architecture of the molecular assemblies. Electrostatic repulsion and the loss of entropy may prevent oligomerization processes, and the example presented here indicates that anionic ligands, van der Waals attraction between adjacent chromophores and the relaxation of strain, due to fused chelate rings in monomeric subsystems, may lead to the preferential formation of oligomeric species.

Table 3 Crystal data, data collection and refinement parameters for complexes $[\text{Cu}(\text{L}^1)] \cdot 2\text{H}_2\text{O}$ and $[\text{Cu}_2(\text{L}^1)_2] \cdot 6\text{H}_2\text{O}$

	$[\text{Cu}(\text{L}^1)] \cdot 2\text{H}_2\text{O}$	$[\text{Cu}_2(\text{L}^1)_2] \cdot 6\text{H}_2\text{O}$
Formula	$\text{C}_6\text{H}_{16}\text{CuN}_4\text{O}_4$	$\text{C}_{12}\text{H}_{36}\text{Cu}_2\text{N}_8\text{O}_{10}$
Formula weight	271.8	579.6
Crystal system	Orthorhombic	Monoclinic
Space group	$P2_12_12_1$	$P2_1/c$
T/K	230	295
$a/\text{\AA}$	7.660(4)	10.977(5)
$b/\text{\AA}$	19.209(3)	15.243(4)
$c/\text{\AA}$	7.265(4)	13.878(4)
$\beta/\text{^\circ}$		100.53(3)
$V/\text{\AA}^3$	1069.1(9)	2282(1)
Z	4	4
$\mu(\text{Mo-K}\alpha)/\text{cm}^{-1}$	20.46	19.28
Total reflections	1066	3965
Unique reflections	930	2612
R	0.044	0.046
R'	0.051	0.044

Experimental

Materials, measurements and computation

The compounds H_2L^1 and $[\text{Cu}(\text{L}^1)] \cdot 2\text{H}_2\text{O}$ were prepared as described.²² UV-vis and IR spectra (KBr pellets) were measured on Specord M40 and 75IR (Carl Zeiss) instruments, respectively, EPR spectra on a Bruker ESP300E spectrometer at 9.4635 GHz as approximately 1 mmol dm⁻³ frozen solutions in DMF-water (1:1) at 120 K. The MOMEMC suite of programs²³ and force field¹⁸ were used for molecular mechanics calculations.

Syntheses

A mixture of single crystals of $[\text{Cu}(\text{L}^1)] \cdot 2\text{H}_2\text{O}$ and $[\text{Cu}_2(\text{L}^1)_2] \cdot 6\text{H}_2\text{O}$ was obtained from a saturated aqueous solution (*ca.* 5×10^{-2} mol dm⁻³) of a microcrystalline sample of $[\text{Cu}(\text{L}^1)] \cdot 2\text{H}_2\text{O}$ ²² (Calc. for $\text{C}_6\text{H}_{16}\text{CuN}_4\text{O}_4$: C, 26.52; H, 5.93; N, 20.62. Found: C, 26.3; H, 6.10; N, 20.50%) to which was carefully added a layer of acetone or acetonitrile; the closed flask was allowed to stay at ambient temperature for several days. Purple needles (the monomer) and purple cubes (the dimer) were separated manually. The ratio of isolated monomer to dimer depended on the concentration and temperature; increasing concentrations and decreasing temperatures favor dimer formation. $[\text{Cu}(\text{L}^1)] \cdot 2\text{H}_2\text{O}$: vis (H₂O) $\tilde{\nu}_{\text{max}} = 18900 \text{ cm}^{-1}$, $\varepsilon = 152 \text{ dm}^3 \text{ mol}^{-1} \text{ cm}^{-1}$; reflectance spectrum $\tilde{\nu}_{\text{max}} = 18800 \text{ cm}^{-1}$, EPR $g_{\parallel} = 2.179$, $g_{\perp} = 2.060$, $A_{\parallel}(\text{Cu}) = 207 \times 10^{-4} \text{ cm}^{-1}$; IR (KBr, cm⁻¹) 3400 (sh) (H₂O), 3300w, 3250m, 3133w (all N–H) and 1593vs (amide). $[\text{Cu}_2(\text{L}^1)_2] \cdot 6\text{H}_2\text{O}$: reflectance spectrum $\tilde{\nu}_{\text{max}} = 18200 \text{ cm}^{-1}$; IR (KBr, cm⁻¹) 3400m (br) (H₂O), 3230m (br), 3135w (both N–H), 1613vs, 1554s (both amide).

Crystal structure determination

Single crystals of suitable dimensions were mounted on glass fibers and data collection was performed on a Rigaku AFC7S diffractometer using graphite monochromated Mo-K α radiation ($\lambda = 0.71069 \text{ \AA}$). The data were collected at 294 K, using 2 θ scans to a maximum of 50.0°. The intensities of three representative reflections were measured after every 150. No decay correction was applied; intensity data were corrected for Lorentz-polarization in both cases; an absorption correction was made in the case of the monomer and a secondary extinction coefficient in the case of the dimer. The crystal data, data collection and refinement parameters are summarized in Table 3. The structures were solved by direct methods using the

SIR 92 suite of programs.²⁴ The non-hydrogen atoms were refined anisotropically. Hydrogen atoms of the water molecules were refined isotropically, the rest were included in fixed positions. All calculations were performed using the TEXSAN crystallographic software package.²⁵

CCDC reference number 186/1665.

See <http://www.rsc.org/suppdata/dt/1999/4099/> for crystallographic files in .cif format.

Acknowledgements

Generous financial support by the German Science Foundation (DFG), the Bundesministerium für Bildung und Forschung (BMBF) and the Fonds of the Chemical Industry (FCI) is gratefully acknowledged. This project has also been supported by the Royal Society of Chemistry and the Foundation of Basic Research, the Department of International Cooperation of the Ministry of the Ukraine for Science and Technology.

References

- D. E. Fenton and H. Okawa, in *Perspectives on Bioinorganic Chemistry*, eds. R. W. Hay, J. R. Dilworth and K. B. Nolan, JAI Press Ltd., London, 1993.
- K. D. Karlin, Z. Tyeklar and A. D. Zuberbühler, in *Bioinorganic Catalysis*, ed. J. Reedijk, Marcel Dekker, New York, 1993.
- E. I. Solomon, U. M. Sundaram and T. E. Machonkin, *Chem. Rev.*, 1996, **96**, 2563.
- D. E. Fenton, in *Transition Metals in Supramolecular Chemistry*, eds. L. Fabbrizzi and A. Poggi, Kluwer, Dordrecht, 1994.
- T. A. Kaden, in *Transition Metal in Supramolecular Chemistry*, eds. L. Fabbrizzi and A. Poggi, Kluwer, Dordrecht, 1994.
- J.-M. Lehn, *Supramolecular chemistry: Concepts and perspectives*, VCH, Weinheim, 1995.
- N. D. Chasteen and R. L. Belford, *Inorg. Chem.*, 1970, **9**, 169.
- Y. Kajikawa, T. Sakurai, N. Azuma, S. Kohno, S. Tsuboyama, K. Kobayashi, K. Mukai and K. Ishizu, *Bull. Chem. Soc. Jpn.*, 1984, **57**, 1454.
- P. Comba, T. W. Hambley, G. A. Lawrence, L. L. Martin, P. Renold and K. Várnagy, *J. Chem. Soc., Dalton Trans.*, 1991, 277.
- P. V. Bernhardt, P. Comba, T. W. Hambley, S. S. Massoud and S. Stebler, *Inorg. Chem.*, 1992, **31**, 2644.
- P. Comba, in *Intermolecular Interactions*, eds. W. Gans and J. C. A. Boeyens, Plenum Press, New York, 1998.
- P. Comba, *Coord. Chem. Rev.*, 1999, **182**, 343.
- J. C. Colin, T. Mallah, Y. Journaux, F. Lloret, M. Julve and C. Bois, *Inorg. Chem.*, 1996, **35**, 4170.
- P. Comba, T. W. Hambley, M. A. Hitchman and H. Stratemeier, *Inorg. Chem.*, 1995, **34**, 3903.
- P. Comba, W. Goll, B. Nuber and K. Várnagy, *Eur. J. Inorg. Chem.*, 1998, 2041.
- P. Comba, S. P. Gavish, R. W. Hay, P. Hilfenhaus, Y. D. Lampeka, P. Lightfoot and A. Peters, *Inorg. Chem.*, 1999, **38**, 1416.
- C. K. Johnson, ORTEP, A Thermal Ellipsoid Plotting Program, Oak Ridge National Laboratory, Oak Ridge, TN, 1965.
- J. E. Bol, C. Buning, P. Comba, J. Reedijk and M. Ströhle, *J. Comput. Chem.*, 1998, **19**, 512.
- P. Comba and P. Hilfenhaus, *J. Chem. Soc., Dalton Trans.*, 1995, 3269.
- P. Comba, *Coord. Chem. Rev.*, 1999, **185**, 81.
- P. Comba and T. W. Hambley, *Molecular Modeling of Inorganic Compounds*, VCH, Weinheim, 1995.
- H. Ojima and K. Yamada, *Nippon Kagaku Zasshi*, 1968, **89**, 490.
- P. Comba, T. W. Hambley, N. Okon and G. Lauer, MOMEMC, a molecular modeling package for inorganic compounds, CVS, E-mail:cvs@t-online.de, 1997.
- A. Altomare, M. C. Burla, M. Camalli, M. Cascarano, C. Giacovazzo, A. Gugliardi and G. Polidori, *J. Appl. Crystallogr.*, 1993, **26**, 343.
- TEXSAN, Crystal Structure Analysis Package, Molecular Structure Corporation, Houston, TX, 1985 and 1992.